

Error Suppression For Continuous Time Quantum Computing

Tom O'Leary

Level 4 Project, MSci Natural Sciences

Supervisors: Professor V. Kendon,

Dr N. Chancellor

Department of Physics, Durham University

Submitted: April 22, 2020

Continuous time quantum computing is an alternative to the widely pursued circuit model, capable of achieving the same computational speed ups over classical computing. It has the added benefit of being a more feasible near term choice for physical implementation. Computation proceeds under time evolution of a Hamiltonian which encodes the target problem. This Hamiltonian can be subject to misspecification error, such that it no longer accurately represents the desired problem.

This thesis investigates an error suppression scheme which aims to reduce the effects of misspecification error by encoding the Hamiltonian describing the problem. The maximum independent set problem, mapped to an Ising model configuration such that it is suitable for use with adiabatic quantum computing, is used as a target problem. Instances of the problem are solved by constructing encoded Hamiltonians subject to varying levels of error. Errors are modelled as small perturbations drawn from a uniform distribution on the Hamiltonian parameters. The scheme is effective and upon careful selection of encoding parameters led to reductions of failure probability of up to 97%. With further refinements in the process of choosing optimal encoding parameters, the scheme presents a promising method for error suppression.

Contents

1. Introduction	3
2. Background	4
A. Quantum computing	4
1. History	4
2. Qubits	4
3. Discrete time quantum computation	5
B. Continuous time quantum computing	6
1. Adiabatic quantum computation	6
2. Quantum walk	7
C. Error correction in quantum computing	9
D. Error correction in the continuous time case	10
1. Errors in adiabatic quantum computation	11
2. Errors in quantum walk computation	13
3. The maximum independent set problem	14

3. Methods	16
4. Results	18
A. Error suppression with quantum statics	18
1. The $n = 3$ maximum independent set instance	18
2. The $n = 5$ maximum independent set instance	20
3. Problem parameter scaling	22
B. Solving instances of the maximum independent set with quantum dynamics	22
1. Adiabatic quantum computing	22
2. Quantum walk	24
5. Discussion	25
6. Conclusions	27
Acknowledgments	28
References	28
A. Calculation of uncertainties	31
B. Supplementary figures	32

1. INTRODUCTION

Classical computing describes the computational model which has discrete binary variables at its foundation: 0s or 1s. The technology underpinned by this model has advanced steadily over the last century although this rate of advance could soon slow as a result of meeting fundamental limits imposed by the laws of physics [1]. However, phenomena from the same area of physics that place limitations on classical computing could be used to develop a fundamentally different paradigm of computing.

The paradigm is quantum computing and theory predicts that it could be used to achieve significant performance improvements over classical computing for certain problems. These performance improvements have been displayed with regards to specific mathematical problems, for example finding prime factors of an integer [2] and searching an unstructured database [3]. These improvements have direct application, for example, the cryptographic schemes securing much of the communication necessary for internet banking rely on the difficulty of finding prime factors of integers using classical computation, a difficulty not shared by a suitably powerful quantum computer.

The most widely studied model of quantum computing is the circuit model, where algorithms are implemented through the successive action of quantum gates on quantum bits or qubits. Analogously, classical computation involves gates acting on bits. In both contexts gates output the result of a particular operation on the input bits. There are, however, alternative models of quantum computation. Considering the action of gates on qubits as a sequence of operations occurring discretely in time, an alternative is quantum computation occurring continuously over time, where a problem is encoded into a physical system which is then evolved such that its final state provides a solution to the problem. This model looks to be a near term solution to the problem of physically realising quantum computing. The first commercially available quantum computer implements a particular type of continuous time quantum computing [4], allowing for the possibility of experimental work to be done. As such this thesis will focus on continuous time quantum computing.

The particular area of focus will be error correction. If quantum computers are to be physically realised they must be done so taking into account the instability of the hardware being used for computation. Qubits are very sensitive to external noise, additionally, it is very difficult to directly check if one has been affected by noise during computation, as the act of direct measurement leads to a collapse of the system's wavefunction, losing the quantum nature of the computational resource. Difficulties are presented by error correction for both the discrete and continuous time models of computation, although the exact nature of errors can differ.

This thesis will be in two parts: a description of the necessary background information to gain an understanding of continuous time quantum computing will be given in the first, this will include the errors it is subject to and a particular scheme to suppress these errors. The second part will take this scheme and adapt it for use with a problem from graph theory called the maximum independent set problem. It is very hard for a classical computer to solve arbitrary instances of this problem [5]. The effectiveness of the scheme as a scalable method for error suppression will be assessed in the context of this problem.

2. BACKGROUND

A. Quantum computing

1. History

Quantum computing's initial appearance came with the introduction and development of the quantum Turing machine by Benioff [6, 7] and Deustch [8] in the early 1980s, a quantum analogue to the abstract model of computation which led to the development of much of classical computing. Additionally, in 1982 Feynman asked the question as to what the nature of a computer that could accurately simulate nature would be [9]. He concluded that due to the exponential growth of the size of physical systems, it would not be feasible for a classical computer, a quantum machine would need to be used. The next few years saw the introduction of algorithms that could be run on a quantum computer that, while reaching a solution exponentially faster than any classical algorithm, were of little apparent practical application.

This changed with Shor's algorithm in 1994 for finding the prime factors of an integer [2], which also produced an almost exponential speed up over the best known classical algorithm but also had direct practical applications. The difficulty of the problem of finding prime factors formed the basis for the security of modern cryptography, for example the RSA cryptosystem used for much of modern secure data transmission. Although a physical quantum computer large enough to use the algorithm for practically large enough numbers has still not been developed, the potential of such a physical machine was established. This was shortly followed in 1995 with an algorithm by Grover [3] for searching an unstructured database in a time proportional to the square root of the size of the database, where the best classical algorithms achieve a time proportional to the size of the database. Furthermore, this was shown by Bennet et al. [10] to be the optimal scaling for searching such a database using a quantum algorithm. The same year Schumacher produced a quantum analogue to Shannon's noiseless coding theorem, helping establish the field of quantum information theory [11], although no analogue for the noisy coding theorem, which would be useful for error correction purposes, has been produced yet.

The years following 2000 have seen much work done towards the physical realisation of quantum computing. This includes small scale experimental demonstrations of the most well-known quantum algorithms [12, 13].

2. Qubits

Unlike classical bits which can represent either 0 or 1, during computation, qubits can be thought of as simultaneously being in a combination of 0 and 1. Denoting the possible single qubit states as $|0\rangle = \begin{pmatrix} 1 \\ 0 \end{pmatrix}$, $|1\rangle = \begin{pmatrix} 0 \\ 1 \end{pmatrix}$ a general qubit $|\psi\rangle$ can be described:

$$|\psi\rangle = \alpha|0\rangle + \beta|1\rangle, \quad (1)$$

where α and β are related to the probability of the qubit, when measured, being a $|0\rangle$ or $|1\rangle$. This in itself is very different to the classical case, but the reason that a quantum computer can

potentially outperform a classical computer is largely down to the way a quantum system grows with additional particles and the resulting increase in computational resources. Introducing a second qubit into the system will lead to a total of 4 possible states to work with, three will mean 8 total states, in general n qubits will lead to 2^n total possible states, so for 50 qubits there are $2^{50} = 1125899906842624$ total states to use simultaneously during computation.

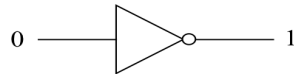
As quantum states, qubits also have the possibility of becoming *entangled* with each other. A system of particles is said to be entangled if the state of each individual particle cannot be described without reference to the other particles in the system. A two qubit example would be the *Bell state*:

$$|\psi\rangle = \frac{1}{\sqrt{2}}(|00\rangle + |11\rangle), \quad (2)$$

where measurement of one qubit will yield 0 or 1 with probability 1/2, however, measurement of the second qubit will always yield the same result as the first.

3. Discrete time quantum computation

The following section is intended to provide a brief introduction to discrete time quantum computation, so that the continuous time counterpart, with no clear classical analogue, can be at least placed in some context for the purposes of intuition. This will consist of comparing the action of a gate on a single classical bit and a single quantum bit. To start with, consider the classical NOT gate, this takes a classical bit to its complement and is drawn in circuit diagram notation as:



Denoting the quantum analogues to the classical 0s and 1s, the single qubit states $|0\rangle$, $|1\rangle$, consider the quantum NOT gate, diagrammatically this has the action:

$$|0\rangle \xrightarrow{\oplus} |1\rangle$$

The action of the NOT gate on a qubit in superposition would then be:

$$\alpha|0\rangle + \beta|1\rangle \xrightarrow{\oplus} \alpha|1\rangle + \beta|0\rangle$$

Denoting a general initial state as $|\Psi_0\rangle$ and a general quantum gate as \hat{U} , then the output state of the computation would be:

$$|\Psi\rangle = \hat{U}|\Psi_0\rangle, \quad (3)$$

where the only constraint on \hat{U} is that it can be represented by a *unitary* matrix, a matrix with the property $\hat{U}^\dagger \hat{U} = I$. So the system evolves through application of a gate at each discrete time step.

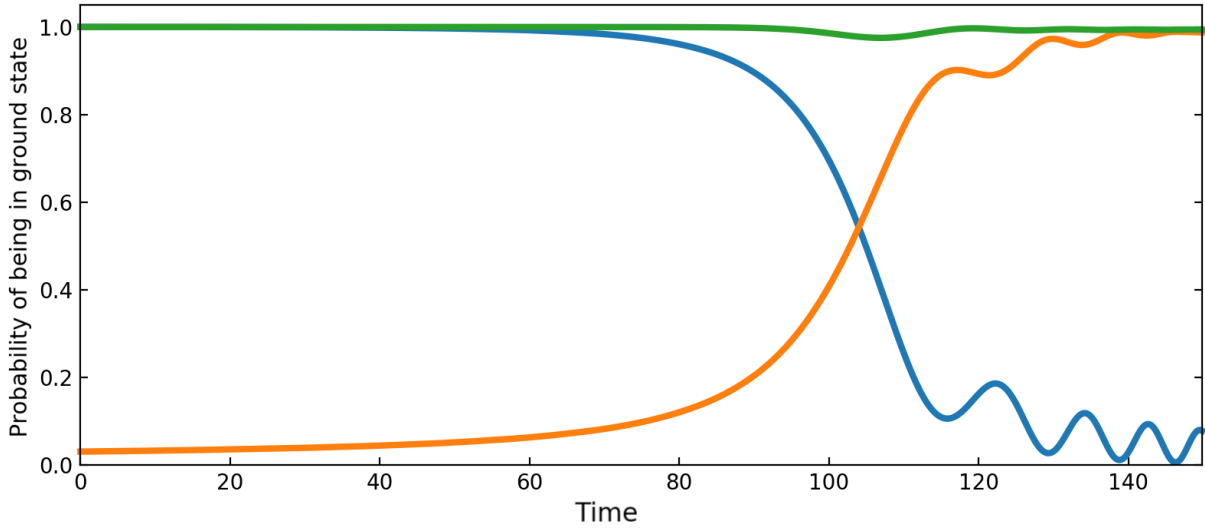


FIG. 1: The probability of being in the ground state of: green: whole Hamiltonian, blue: the initial Hamiltonian, orange: the problem Hamiltonian.

B. Continuous time quantum computing

The main difference to the discrete time case comes in the form of time evolution that takes place. With continuous time computation, instead of the successive application of quantum gates on a state at discrete time steps, the form of a state's time evolution is such that it satisfies the Schrödinger equation for a time dependent Hamiltonian $H(t)$:

$$H(t) |\Psi\rangle = i \frac{\partial}{\partial t} |\Psi\rangle, \quad (4)$$

where the units are such that $\hbar = 1$. This is the equation that governs the time evolution of a quantum system, so continuous time computation can be thought of as encoding the target problem into a physical system, then allowing the natural physical evolution of the system to reach the problem solution. This general description becomes more concrete with the description of specific continuous time algorithms.

1. Adiabatic quantum computation

First introduced in 2000 [19] the adiabatic quantum computation algorithm makes use of the adiabatic theorem from quantum mechanics. This essentially states that for a smoothly varying time dependent Hamiltonian with a non-zero gap between the two lowest energy states, if the Hamiltonian is initialised in its ground state and slowly varied, at some sufficiently long later time the system will remain in the ground state of the varied Hamiltonian with a high probability. The minimisation of the system energy involved in this process means adiabatic quantum computation is particularly suited to solving optimisation problems. The application to computation comes by using a Hamiltonian of the form:

$$H(t) = A(t)H_{init} + B(t)H_{prob}, \quad (5)$$

where $A(0) = 1, B(0) = 0$ and $A(t_f) = 0, B(t_f) = 1$ are the conditions on the real valued coefficients which control the balance of Hamiltonians by smoothly varying between the start of computation until the completion at t_f . H_{init} is some easy to initialise starting Hamiltonian and H_{prob} is a Hamiltonian chosen such that its ground state solves the target problem. Fig. 1 shows how the probability of being in the ground state of each Hamiltonian in Eq. (5) changes throughout a run of adiabatic quantum computation.

A common choice for a physical system to encode the problem into is the *Ising model*, first introduced in the 1920s as a model for ferromagnetism. It involves spins being placed at points on a grid with interactions only considered between neighbouring spins, as shown on the left in Fig. 3. There are efficient mappings for many well-known optimisation problems to the model [5]. In the case of the Ising model the Hamiltonians used are:

$$H_{init} = -h \sum_i^N \sigma_i^x \quad (6)$$

$$H_{prob} = H_{Ising} = \sum_{\langle i,j \in \mathcal{E} \rangle} J_{ij} \sigma_i^z \sigma_j^z + \sum_{i=1}^N h_i \sigma_i^z, \quad (7)$$

where σ are Pauli matrices representing quantum spins, h, h_i are the local transverse and longitudinal field strengths respectively. The coupling strength between spins are specified by J_{ij} and \mathcal{E} is the set of i, j pairs with a non-zero coupling. H_{init} has as its ground state an equally weighted linear combination of all the basis states of H_{Ising} . The choice of parameters h_i, J_{ij} specify the problem instance and will be referred to as the *problem parameters*.

While the choice of Hamiltonian determines the particular problem being targeted, the parameters $A(t), B(t)$ determine the performance of the algorithm. $A(t) = 1 - (t/t_f), B(t) = t/t_f$ is a choice which will yield the correct answer but not necessarily efficiently. In [16] it was shown that adiabatic quantum computation could be used to achieve a speed up for searching approximately equivalent to Grover's quadratic speed up but only in the case coefficients which were non-linear in time were used i.e. the rate of variation of the Hamiltonian increased and decreased at different points during the computation. In the case of adiabatic quantum computation this corresponded to slowing down when the energy between the ground and first excited states was at its smallest throughout computation.

Also worth consideration is *quantum annealing*, which can be considered to be quite similar to adiabatic quantum computation [20], a key difference is that there is no requirement for the system to remain in a ground state for during computation, with jumps to excited states occurring, which are partly negated by cooling.

2. Quantum walk

The quantum walk exists in both discrete [14] and continuous time forms [15]. The former can be viewed as a quantum analogue to the classical random walk, where the coin being flipped at each time step, as well as the walker who's direction is being determined are replaced by quantum states subject to the effects of interference. These effects lead to a different probability distribution of final positions as shown in Fig. (2).

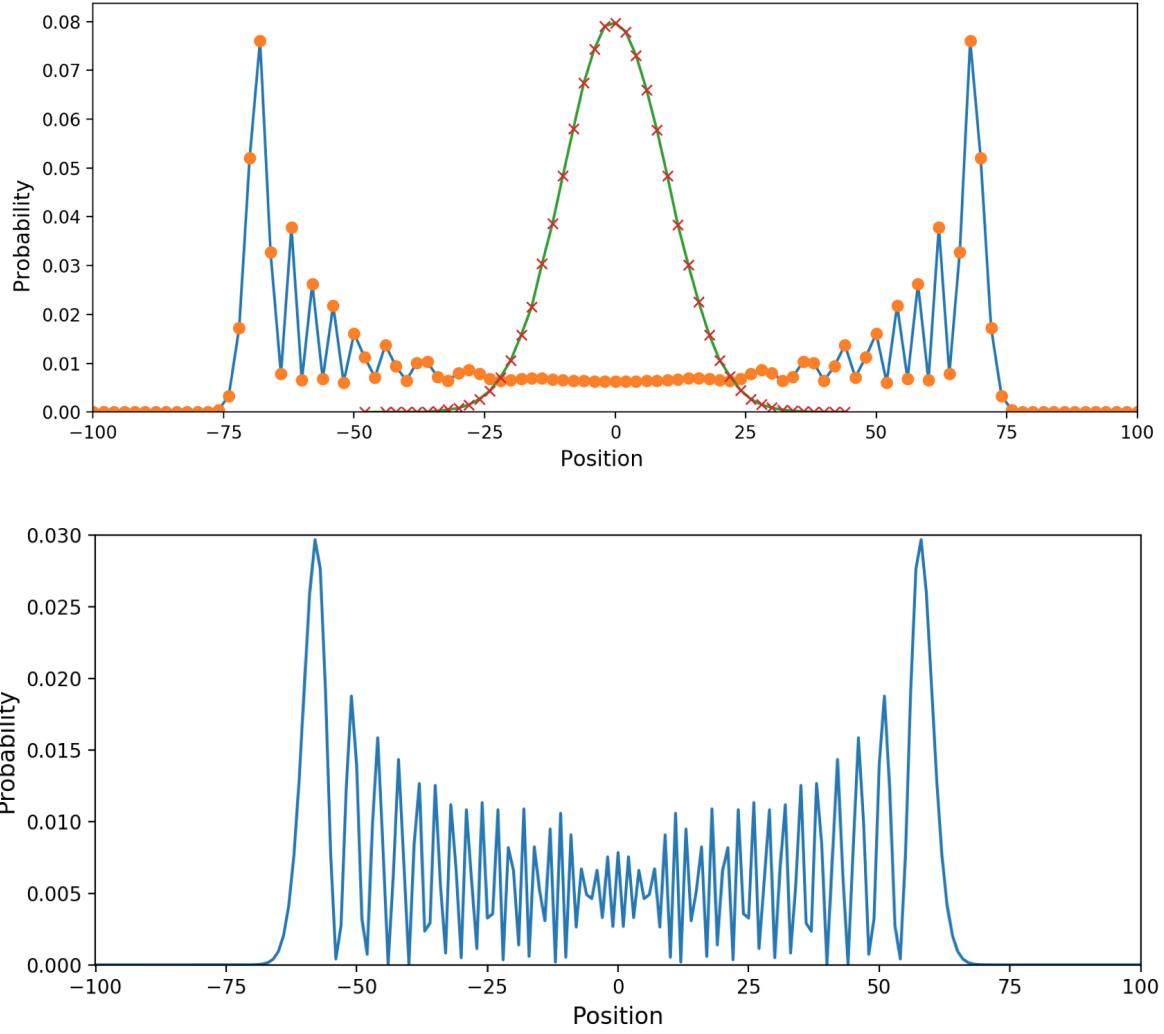


FIG. 2: Top: the probability of a walker being at a particular final position for a classical random walk: crosses and a discrete time quantum walk: dots. Bottom: a continuous time quantum walk, from a walker beginning at the centre, with a hopping rate of 0.5 over 61 timesteps.

The Hamiltonian for the continuous time quantum walk can be defined by considering the *adjacency matrix* of an undirected graph G . A graph is a mathematical structure with vertices connected by edges, an example graph can be seen in Fig. 3, with three vertices (black circles) connected by two edges (lines). If G has vertices $\{j\}$ then the adjacency matrix will have an entry of 1 if there is an edge between j and k else 0. An undirected graph is as opposed to a directed graph where there might be an edge from j to k but not k to j (Although the distinction isn't central to this thesis).

As this matrix will be symmetric and have real entries it meets the condition of unitarity and as such can be used to define a valid Hamiltonian. Here the choice of Hamiltonian is time independent, which means Eq. (4) can be analytically solved, giving the result for the time evolution of the initial state:

$$|\psi(t)\rangle = e^{-i\hat{H}t} |\psi(0)\rangle, \quad (8)$$

which turns out to be similar to Eq. (3). The continuous time quantum walk has been ap-

plied to a range of problems, including formulation as a search algorithm capable of matching the speedup yielded by Grover's [16], finding the ground states of spin glasses [17] and has been proven to be a form of universal computation [18]. It was shown that, when used for search, adiabatic and quantum walk computation can be considered as endpoints of a single hybrid algorithm which meant the balance of each algorithm could be controlled during the computation [16]. In certain cases this led to better results than a single choice. Additionally, the work finding the ground states of spin glasses is notable as it uses a quantum walk to determine the ground state of an instance of the Ising model . It was shown the choice of Hamiltonian in Eq. (8) necessary for doing so was the transverse Ising model Hamiltonian: Eq. (5) with coefficients $A = B = 1$ with Eq. (6) and Eq. (7) as initial and problem Hamiltonians respectively. In this case h in Eq. (6) is referred to as the hopping rate of the quantum walk.

C. Error correction in quantum computing

One of the main challenges to the physical realisation of quantum computing, in both the discrete and continuous time cases, is the instability of qubits as a way of storing information. The specific instability will depend on the model of computation being implemented, but the causes of the instability are similar. A physical quantum computer will necessarily have to be an open system, coupled to the environment, leading to the introduction of external noise. This noise can lead to a qubit changing state from the one intended to be used for computation e.g. flipping a $|0\rangle$ to a $|1\rangle$. Even supposing that every qubit being used could be guaranteed to be reliable, this external noise could affect the apparatus being used to control the qubits. Leading to systematic errors that could affect the specification of the problem being solved or the measurement of qubits to obtain the results of computation. Additionally it is not possible to directly check if a qubit has been subject to error because of the effect of *wavefunction collapse*, where the 'measurement' of a qubit will cause it to collapse from a quantum system with multiple possible outcomes, to a classical system with a definite state, this process is irreversible and destroys the quantum nature required for computation. A further key difficulty is that, unlike classical bits which can be subject to a single type of error: the bit flip, a qubit is described by parameters defined over a continuum, to see this consider an alternative representation of Eq. (1) :

$$|\psi\rangle = \cos\left(\frac{\theta}{2}\right)|0\rangle + e^{i\phi}\sin\left(\frac{\theta}{2}\right)|1\rangle, \quad (9)$$

where θ, ϕ are the continuous parameters, any change in which leads to a different quantum state. There are already several well-known, robust error correction schemes for classical computing [21], so it would be useful if these could be adapted for quantum computing. These schemes often rely on the ability to encode classical bits using repetition, so that in the event of an error, ideally, the most of the repeated bits remain in the original correct state and this state can be restored using a majority vote. However, the ability to repeat or clone bits doesn't carry over to the quantum case due a fundamental result in quantum mechanics known as the *No Cloning Theorem*, which shows that nature forbids a quantum state from being duplicated [22].

Despite the challenges raised, quantum error correction schemes have been developed. Fortunately the difficulty posed by the continuous nature of quantum errors can be addressed by the *digitisation* of quantum errors [23]. Where despite being described by continuous parameters, every quantum error can be reduced to the action of a discrete set of operations, so arbitrary errors can be protected against by protecting against this set. These operations are the bit flip, which is the same as the classical case, and the phase flip, which doesn't have a classical analogue and in a simple case has the action: $|\psi\rangle = \alpha|0\rangle + \beta|1\rangle \rightarrow \alpha|0\rangle - \beta|1\rangle$.

The first error correction scheme was proposed by Shor in 1995 [24] and is aimed at overcoming the effects of decoherence, which inevitably occurs given time for an open quantum system. Where the qubits being used for computation entangle with the environment, therefore corrupting the computation. It does this by constructing each qubit used for information processing, a logical qubit, with 9 physical qubits, of which the computer is actually constructed. The physical qubits used for a logical qubit are entangled together, spreading the information across multiple states, exploiting redundancy in a similar manner to classical repetition codes, but in the context of a quantum system. This makes it possible to check whether a logical qubit was subjected to an error, and which error it was subjected to, without directly measuring the qubit and therefore avoiding compromising the information.

So, as the problem of digitising quantum errors was solved, Shor's scheme introduces a technique that can address the difficulties introduced by the No Cloning theorem and wavefunction collapse. Following Shor's code there have been several, increasingly general, error correction schemes constructed. Derived from a class of classical error codes called *linear codes*, the Calderbank-Shor-Steane or *CSS* codes is a class of quantum codes that was introduced in 1996 [25, 26] which is capable of detecting and correcting against both bit and phase flip errors. An even more general class of codes, that the CSS codes turned out to be a subclass of, are *stabiliser codes* [27]. The use of these codes is similar to that of the Shor code: entangle the original information with additional, redundant qubits, 'spreading' the information across several states, then to check if an error has occurred, measure these redundant qubits using a stabiliser operator. Whether a stabiliser code only tells you if an error has occurred or if it also specifies what type of error and on which qubits depends on the particular code used, often with more redundant qubits required for more information. Construction of working stabiliser codes is a key challenge. One such method of construction uses *Surface Codes*, which generate larger codes by patching together working smaller codes. This option is currently widely pursued as a method to experimentally implementing quantum error correction due to its suitability to being scaled to larger systems [28]. In fact, due to the large qubit overhead introduced by error correction schemes, this scaling to larger systems is a key challenge to experimental implementation of quantum computing [29].

D. Error correction in the continuous time case

Decoherence remains a source of error in the continuous time case, with the coupling to an environment placing a limit on the time an algorithm could be run for left unchecked. Using the example of performing a search, eventually the effects of decoherence will keep the system in such a state that a continuous time quantum algorithm will be doing the same thing as classical

random guessing [16]. Although in general this can be countered by simply performing repeat runs of the algorithm, with more runs required the further a success probability is reduced by errors. In cases where high efficiency is a goal, this is not always a viable strategy. A strategy for protecting against errors will depend on the type of error. As the problems to solve are encoded into physical systems, the fragility of these quantum systems is still a cause for error. Thermal noise can lead to unwanted variation in the parameters used to encode the problem, examples could be the coupling strengths between qubits or the state of the qubits themselves. Again, looking at specific continuous time algorithms will be useful for gaining an understanding.

1. Errors in adiabatic quantum computation

Adiabatic evolution sees an initial Hamiltonian varied slowly enough so that if the system is initialised in this Hamiltonian's lowest energy state, it will end up in the lowest energy state of the final Hamiltonian after variation. Ideally, the system remains in the lowest energy state of each Hamiltonian produced by each slight variation. Fortunately there is a level of inbuilt protection against noise for this condition. Noise which isn't great enough to provide enough energy to the system so that it is excited to the 1st excited state, should not affect the computation as the system will remain in the ground state [30].

In 2008 Jordan, Farhi and Shor [31] proposed a method for combatting unwanted changes in the Hamiltonian as the result of noise. They encoded the Hamiltonian using the stabiliser code formalism and adding additional terms to this encoded Hamiltonian that essentially introduced an energy penalty for errored states. It would 'cost' the system more energy to change to an errored state and so it would be more likely to stay in the correct, lower energy state. This is a form of error suppression rather than correction, it doesn't remove errors from the system, just reduces the probability of them occurring.

However, in 2013 Young and Sarovar [32] showed that using stabiliser codes for error correction with adiabatic quantum computation led to uncorrectable errors. Essentially, the Hamiltonian would be encoded according to the stabiliser formalism and computation would take place. If an error acted on the state, the stabiliser code used would allow for unique identification of what kind of error occurred and on what qubit it occurred, the requirement for error correction. This identification would take place at the end of the computation and the correction could be performed on the end state. But between the error acting and being corrected, the system will have very likely begun evolving in a different manner to that which was intended. Once the error acts on the system it changes its state, so the encoded Hamiltonian will no longer act on the system in a manner such that it solves the desired problem. The evolution of the system could continue perfectly, but it would be subject to a logical error, 'receiving valid instructions but using them to head in the wrong direction'. A solution to this issue that fit into the stabiliser formalism was proposed, that only utilised resources available to adiabatic computation, but was considered unphysical, in part because of the large number of operations required. Suggesting that adiabatic quantum computation and the stabiliser formalism may not be compatible.

The same year another source of error apart from that which could occur during adiabatic evolution was addressed. This was misspecification error for the Ising model in the context of adiabatic quantum computation [33, 34]. Correctly specifying the parameters to experimentally

implement a Hamiltonian for use with adiabatic quantum computing requires very high precision. Even a slight discrepancy could lead to a different system and therefore a different problem being solved. As the starting Hamiltonian is by design easy to implement and the intermediate Hamiltonians don't need to be known, the focus was on the final Hamiltonian, the ground state of which provided the solution to the desired problem. The scheme proposed sought to protect the accuracy of this Hamiltonian through encoding. The encoding scheme duplicated each qubit in the physical implementation of the Hamiltonian, such that each logical qubit was represented by a number of physical qubits. These duplicates were connected by strong ferromagnetic links. These links introduced an energy penalty to the system, so that in the case of an error occurring, it would be energetically preferential for the system to remain in the un-errored state. So this is another form of error suppression. The repetition encoding was also shown to be a particular case of a stabiliser encoding. The encoding process is shown diagrammatically in Fig. 3. The scheme was experimentally tested using a D Wave quantum annealer and was shown to be successful while the assumptions going into the theory, such as small, independently acting errors, held. So error suppression seems possible for adiabatic computation but error correction, which was argued by Young as necessary for large scale computations, may not be possible using the stabiliser formalism.

The scheme as described in [34] was chosen as the start point for further examination of error suppression for continuous time quantum computing. The formalism for the encoding will be described here. Starting with the Ising Hamiltonian being used to encode the problem:

$$H_{Ising} = \sum_{\langle i,j \in \mathcal{E} \rangle} J_{ij} \sigma_i^z \sigma_j^z + \sum_{i=1}^N h_i \sigma_i^z, \quad (10)$$

modelling the misspecification errors as small perturbations on the couplings and local fields:

$$H_{Ising} = \sum_{\langle i,j \in \mathcal{E} \rangle} (J_{ij} + \epsilon_{ij}^J) \sigma_i^z \sigma_j^z + \sum_{i=1}^N (h_i + \epsilon_i^h) \sigma_i^z, \quad (11)$$

The Hamiltonian resulting from use of the protection scheme, the encoded, or 'protected', Hamiltonian is as follows:

$$\overline{H} = \sum_{\langle i,j \in \mathcal{E} \rangle} \sum_k (J_{ij} + \epsilon_{ij,k}^J) \sigma_{i,k}^z \sigma_{j,k}^z - \sum_{i=1}^N \sum_k (h_i + \epsilon_{i,k}^h) \sigma_{i,k}^z + \sum_{i=1}^N \sum_{\langle k,l \in \mathcal{E}_F \rangle} (-J_F + \epsilon_{i,kl}^{J_F}) \sigma_{i,k}^z \sigma_{i,l}^z \quad (12)$$

The duplicates of the original Hamiltonian can be seen in the first two terms in the sums over k . For clarity: a system with 1 duplicate, as depicted in Fig. 3, corresponds to $k = 2$ total Ising blocks. Where an Ising block is the configuration described by Eq. (10) before encoding. $\sigma_{i,k}^z$ denotes the Pauli Z matrix acting on the i th qubit in the k th block, which is equivalent to the Pauli Z matrix on the m th qubit in the system which is enlarged due to the additional duplicate qubits, the map between i, k and m will depend on the choice of qubit labelling.

This duplication could be thought of as having multiple trials of the computation running simultaneously, which in itself will yield a higher success probability through repetition. Intended to improve over this, the duplicates are then connected by ferromagnetic couplings to the other

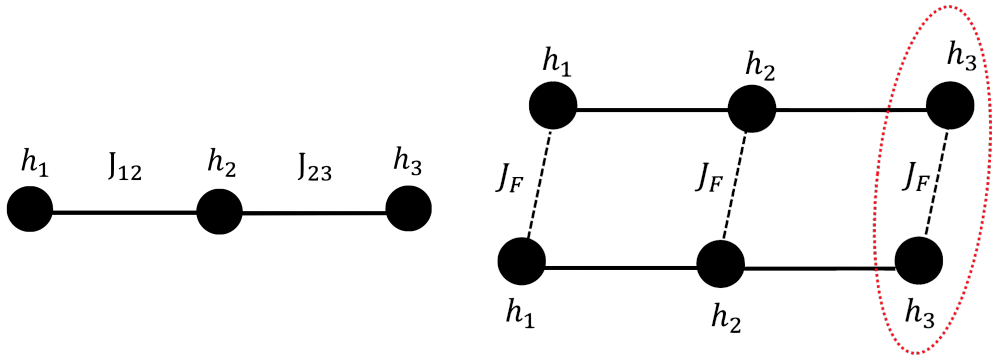


FIG. 3: Left: graphical representation of Ising model, vertices are spins with local field strength h_i , edges are couplings with strength J_{ij} . Right: the left graph after encoding, the dotted lines are strong ferromagnetic links connecting the physical qubits that make up a logical qubit, an example of which is outlined.

copies. The particular choice of coupling for each duplicate is an implementation detail that can affect the effectiveness of the scheme. These couplings can be seen in the third term in Eq. (12), the strength of these is denoted by J_F and in the original work was of the scale of the couplings in the original Ising model J_{ij} . \mathcal{E}_F denotes the edge set which specifies which qubits in each duplicate will be coupled. In the context of the original papers it was suggested that the scheme would be successful in the case that the qubits in the original Ising configuration in each duplicate had a higher connectivity than that between duplicates. For 1 duplicate, $k = 1$, a choice of coupling is a linear chain, this is can be seen in Fig. 3. An additional duplicate, $k = 2$, introduces an additional degree of freedom into the system: how to 'tie' the copies in each logical qubit together. Here this was done in the same way for every logical qubit and was done as shown on the right in Fig. 7. A linear chain as before but extended by one (top), the chain with the first and last qubits coupled with an additional ferromagnetic coupling: a *ferromagnetic loop* (middle) and the chain with an *antiferromagnetic loop* (bottom).

2. Errors in quantum walk computation

As there is no intrinsic energy gap involved with quantum walk computation, the algorithm doesn't have the associated robustness to noise that adiabatic quantum computing does. However, when considering a quantum walk where the system was subject to decoherence, it was suggested that small amounts of decoherence could lead to better results with regards to certain walk parameters, than that would be achieved in a system with no decoherence [35].

In the specific case of performing search [16], the algorithm was shown to be more robust to environmental noise than adiabatic quantum computing. This was in the sense that, if lower success probabilities could be tolerated, the quantum walk would consistently deliver higher success probabilities for a greater range of decoherence.

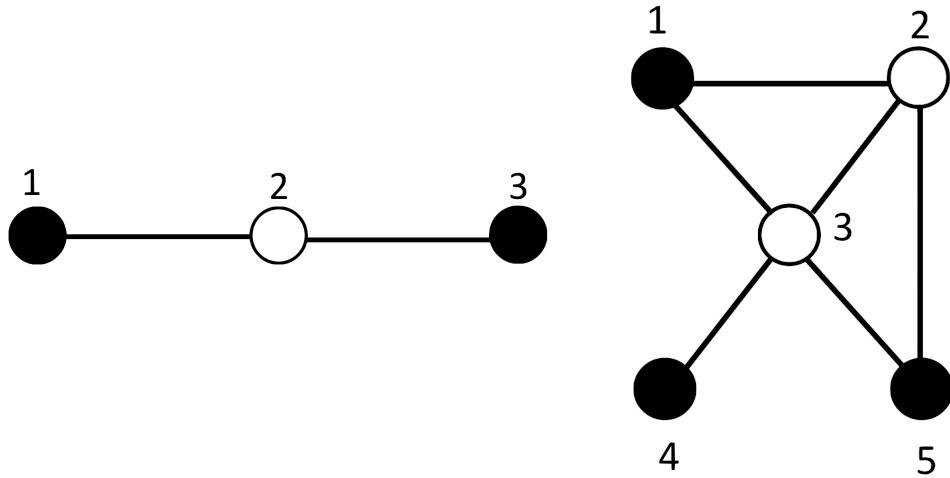


FIG. 4: Maximum independent set solutions for graphs of size left: 3 and right: 5, black and white nodes represent weights 1 and 0 respectively.

3. The maximum independent set problem

The choice of computational problem to investigate the performance of the error suppression scheme was the maximum independent set problem, a problem from graph theory. In our case the graph being considered has vertices which can have weight 0 or 1. An independent set would be a subset of the graph where the assignment of weights is such that no vertices with weight 1 have an edge between them. There can be multiple independent sets of varying sizes for a given graph. The maximum independent set of a graph would be the subset which is an independent set and has the maximum total vertex weight. Although there could be multiple subsets with this maximum weight, this work will refer to 'the' maximum independent set except when explicitly dealing with a problem with degenerate solutions.

But how would one map these problem instances to a problem Hamiltonian for use with adiabatic quantum computing? As this model performs minimisation of a system's energy, we would like the ground state of our problem Hamiltonian to correspond to the maximum independent set. It turns out that the maximum independent set has a fairly natural mapping to the Ising model. For a graph G with vertices V , edges E and adjacency matrix M , with $M_{ij} = 1$ if $(i, j) \in E$ else $M_{ij} = 0$, consider a $n = |V|$ qubit instance of the Ising model, as described in general by Eq. (10). Consider a direct representation of vertex weights 0 and 1 by qubit states $|0\rangle$ and $|1\rangle$. The effect of the $J_{ij}\sigma_i^z\sigma_j^z$ term will be to return $+J_{ij}$ or $-J_{ij}$ if qubits i and j are in the same state: $|0\rangle|0\rangle$, $|1\rangle|1\rangle$ or different states: $|0\rangle|1\rangle$, $|1\rangle|0\rangle$ respectively. This is the independent set condition and applies to any vertices with edges between them. So by setting $J_{ij} = M_{ij}$, the coupling term of the Ising Hamiltonian will result in the lowest energy for a state where no connected qubits have the same state: an independent set. The linear term in the Ising Hamiltonian σ_i^z will return +1 or -1 for a $|0\rangle$ or $|1\rangle$ respectively. So just having this term acting on each qubit would return the lower energy for a state with more qubits in $|1\rangle$, but with no consideration of the connectivity of these qubits. A very well connected $|1\rangle$ qubit would be more likely to break the independent set requirement. Choosing

$$h_i = -\left(\sum_j M_{ij} + M_{ji}\right) + \kappa \quad (13)$$

addresses this: the first term will reward a lower energy for a highly connected qubit in $|0\rangle$ and penalise a highly connected $|1\rangle$ qubit, the second term provides a balance to this, rewarding a state with more qubits in $|1\rangle$ [36].

A benefit of using this Ising model mapping is that the problem Hamiltonian constructed is diagonal, with the i th diagonal element corresponding to the energy of the n bit binary representation of i e.g. $n = 3, i = 5 = 101$ in binary. Assigning each vertex in the problem instance a label, as in Fig. 4, each column in the n bit binary number can be considered to represent the state of a vertex. So the 2^n different bit strings possible for an n bit binary number contain every different possible assignment of weights to the graph. So by simply by constructing the problem Hamiltonian the energy levels of each solution have been obtained. The index of the minimum diagonal element will specify the configuration corresponding to the ground state and will ideally be the maximum independent set. It is important to note this method of obtaining solutions is only practical for smaller system sizes, as the size of the matrix grows as $2^n \times 2^n$.

Two maximum independent set problem instances were used to examine the effectiveness of the protection scheme, these are both shown in Fig. 4. There is an $n = 3$ instance which is the smallest non trivial maximum independent set problem instance. This instance has a single optimal solution which corresponds to a non degenerate ground state in the problem Hamiltonian, this means it is clear to verify if the mapping has been subjected to a notable level of error. The specific Ising Hamiltonian for $n = 3$ mis instance:

$$H_{Ising} = \sigma_1^z \sigma_2^z + \sigma_2^z \sigma_3^z + (-1 + \kappa) \sigma_1^z + (-2 + \kappa) \sigma_2^z + (-1 + \kappa) \sigma_3^z. \quad (14)$$

The $n = 5$ instance presents additional difficulties: the larger problem size and a higher degeneracy of first and second excited states in the Hamiltonian [36]. This second difficulty means there are multiple energy levels close to the ground state that don't correspond to maximum independent set configurations. These could swap with the ground state with errors applied.

The problem has been examined previously in the context of adiabatic quantum computing using a mapping to an Ising Hamiltonian. Choi investigated a more general problem: the maximum weight independent set problem, of which our problem can be considered an example with a constant vertex weight of 1 [37]. Dickson and Amin aimed to show that adiabatic quantum computing wouldn't always necessarily take prohibitively long for solving computationally hard problems [38]. Both of these works were concerned with the runtime of adiabatic evolution required for computation to succeed. The problem being addressed was the existence of a 'first order quantum phase transition' that can occur during adiabatic computation, this leads to a minimum energy gap which decreases exponentially with system size, increasing the problem runtime. Both works remove this phase transition by scaling the problem parameters in the Ising Hamiltonian, leading to an increased minimum gap. Although the application differs, the use of parameter scaling is also examined in this thesis.

Neither of these works directly considered the performance of error suppression on the maximum independent set problem. Sarkoni et al. observed the performance of a physical quantum processing unit in solving instances of the maximum independent set problem in comparison to classical algorithms [39]. They focused on the problem as it is well studied in graph

theory and has been classified as a computationally hard problem in such a way that conclusive results about adiabatic quantum computation's ability to solve the problem would also apply to a range of other problems. They noted that the physical processor was outperformed by simulated annealing, a classical algorithm, as a result of control errors leading to misspecification errors in the parameters encoding the problem Hamiltonian. The qubits in the system were encoded using repetition in a linear chain but for chains much longer considered in this work and a focus more on the overall performance than observing why the encoding worked. The situation was made more complex through the need to format the qubit configuration in such a way it could be effectively used with the physical hardware: minor embedding. Despite this, the work does suggest an application for improvements in the protection scheme.

3. METHODS

The errors being investigated are misspecification errors, where the final Hamiltonian is changed such that it no longer represents the problem it was intended to encode. This was modelled by introducing small perturbations to the parameters that characterised the Ising Hamiltonian and therefore the particular problem instance being solved. These errors were drawn from a uniform distribution in the range between (and including) the positive and negative values of a bound that will referred to as the *error bound*. A uniform distribution was chosen as it reduces the possibility of getting large clusters of small magnitude errors with a small number of very large errors, relative to the bounds on the distribution, that could occur with a normal distribution. Errors were considered on the problem parameters: J_{ij} and h_i so $\epsilon_{i,kl}^{J_F} = 0 \forall i, k, l$ in Eq. (12).

With these errors present, the solution space remains the same: all classical bit strings of length n for a graph with n vertices, each one representing a different assignment of weights to each vertex in the graph. What is affected will be the energy corresponding to each of these solutions in the system described by the Ising Hamiltonian. The ground state of this system may no longer correspond to an optimal solution as the conditions intended to make a maximum independent set energetically preferential are modified. This switching of the system's energy levels such that the lowest energy state configuration no longer corresponds to a maximum independent set is what constitutes a *broken* ground state.

As mentioned, the Ising Hamiltonian has as its diagonal elements the energy of each possible solution to the problem, so simply by constructing this Hamiltonian, subject to errors of a varying magnitude, and observing the ground state, it is possible to determine if the problem has been mis specified. This will be referred to as working in the context of *statics* and will form the majority of the investigation. Then the effect of changing any of the variables going into construction of the problem Hamiltonian can be seen in terms of a yes or no question: is the ground state correct? A consideration in much other work is the nature of the adiabatic evolution. Here it is assumed the evolution proceeds as expected, accurately minimising the energy of the final Hamiltonian but the final Hamiltonian itself may not be accurate. To see how the presence of errors affected the energy levels of the Ising Hamiltonian specifying the problem, the Hamiltonian was constructed with errors on each parameter drawn from a fixed range of the error distribution, the index of the lowest energy state was compared to the expected

solution. This process was repeated over a fixed number of trials with the output being the fraction of trials where the ground state was broken.

An important question to ask is: if the solution to the problem corresponded to the ground state of a system described by this Ising Hamiltonian, once that this Hamiltonian has been encoded as in Eq. (12), what is the form of a correct ground state in the larger system? Where before the ground state would have an n bit binary label, the system is now of size $k * n$ where k is the number of Ising blocks e.g. $k = 2$ in Fig. 3. A correct ground state would be one which had 1 or more of the k blocks in the ground state of the unprotected problem. For the 3 vertex instance in Fig. 4 the ground state of the unprotected problem with $k = 1$ is '101'. With 1 duplicate $k = 2$, there are now multiple correct ground states: 'b₅ b₄ b₃ 101' or '101 b₂ b₁ b₀', b_i is either 0 or 1.

The ideal endpoint of this thesis would be an error suppression scheme for adiabatic quantum computing which required only local information, in the case of the Ising model the coupling and field strengths at each qubit, to determine the optimal input parameters. Such a scheme would likely be efficiently scalable to larger systems. As such, the investigation was started with small problem instances to be able to isolate the effects of the error suppression scheme.

For simulating quantum dynamics an approximation of to a solution of the time dependent Schrödinger equation is used. This involved taking Eq. (8) and considering that the Hamiltonian has time dependence, then:

$$|\psi(t_f)\rangle = \int_0^{t_f} Dt\tau e^{-iH(t)} |\psi(0)\rangle \quad (15)$$

where τ is not a constant and specifies integration in order of increasing time, t_f is the time at the end of evolution. This integral can actually be written as a product of matrix exponentials:

$$\int_0^{t_f} Dt\tau e^{-iH(t)} = \lim_{q \rightarrow \infty} \tau \prod_{j=1}^q e^{-i(t_f/q)H(jt_f/q)}. \quad (16)$$

This result is exact in the limit of infinite q , for finite q , it will provide an approximation to the integral, with an associated numerical error [36]. The larger q is the better the approximation. Putting this together, at a time $k(t_f/q)$:

$$|\psi(kt_f/q)\rangle = \tau \prod_{j=1}^q e^{-i(t_f/q)H(jt_f/q)} |\psi(0)\rangle. \quad (17)$$

The matrix exponential was calculated using a sparse matrix function from the SciPy library for the Python3 language [40]. In this work q was set to 100, the result of Eq. (17) converged to a particular value for values of q much less than 100, so it was a value considered to minimise the numerical error associated with the approximation used.

The hopping rate for the quantum walk was chosen by taking a range of 1000 equally spaced values between 0 and 1, then observing which one led to the maximum success probability when used with the algorithm, this was done for each problem instance.

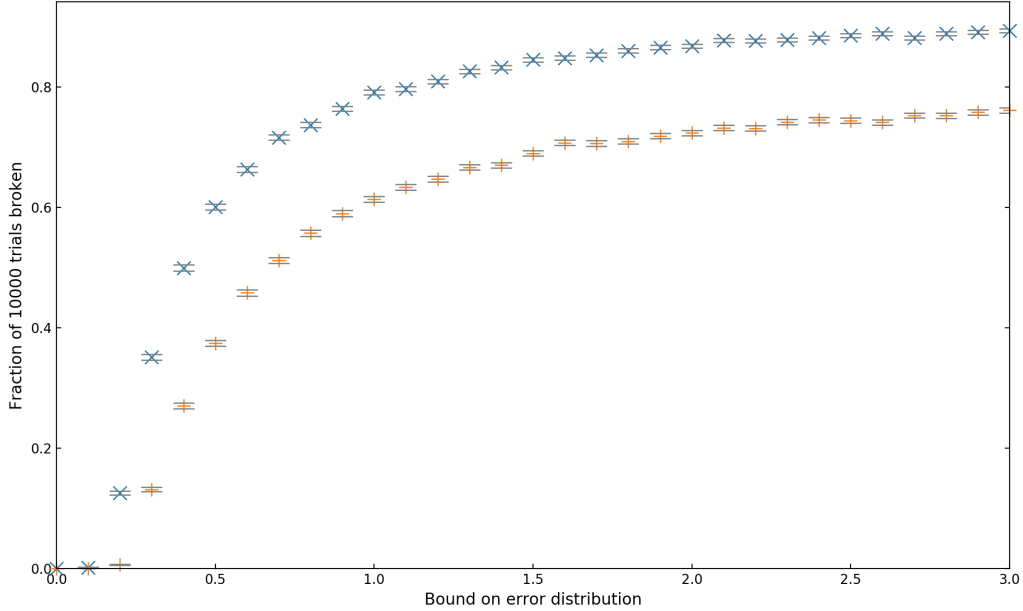


FIG. 5: The fraction of 10000 trials with an incorrect ground for the $n = 5$ (crosses) and $n = 3$ (pluses) problem instances.

4. RESULTS

A. Error suppression with quantum statics

1. The $n = 3$ maximum independent set instance

The $n = 3$ instance solution corresponds to '101' or 5. The fraction of 10000 trials with an incorrect lowest energy state for increasing error bound can be seen in Fig. 5. Initially errors of a higher magnitude were considered, but it was found the fraction of failed trials tended became roughly constant at a limiting error bound of around 3.

The next step was to implement the error suppression scheme introduced in Section 2 D 1. This was done at first using one duplicate, $k = 2$, with a duplicate coupling strength $J_F = 1$. Doing so led to a reduction in the fraction of trials with a broken ground state for all error bounds. Following this positive result it was asked: is it possible to optimise J_F , the only free variable in the scheme with one duplicate, to minimise the number of failed trials? Because of slight ambiguity in the literature, this was investigated for negative and positive values of J_F , the results are shown in Fig. 6. Positive values of J_F correspond to ferromagnetic couplings, negative to antiferromagnetic couplings. Looking at the third term of Eq. (12), $\sigma_{i,k}^z \sigma_{i,l}^z$ will contribute +1 or -1 to a state where the qubits labelled by i, k or i, l are in the same state or different states respectively. So ferromagnetic couplings can be considered to encourage alignment of qubits and antiferromagnetic couplings misalignment. The antiferromagnetic couplings led to the greatest reduction in the fraction of failed trials, the exact improvement can be seen in Table I, corresponding to a 95% decrease.

Fig. 7 shows the effect of adding a further duplicate, $k = 3$, for three different coupling configurations. These configurations were considered for the same range of error bounds, only

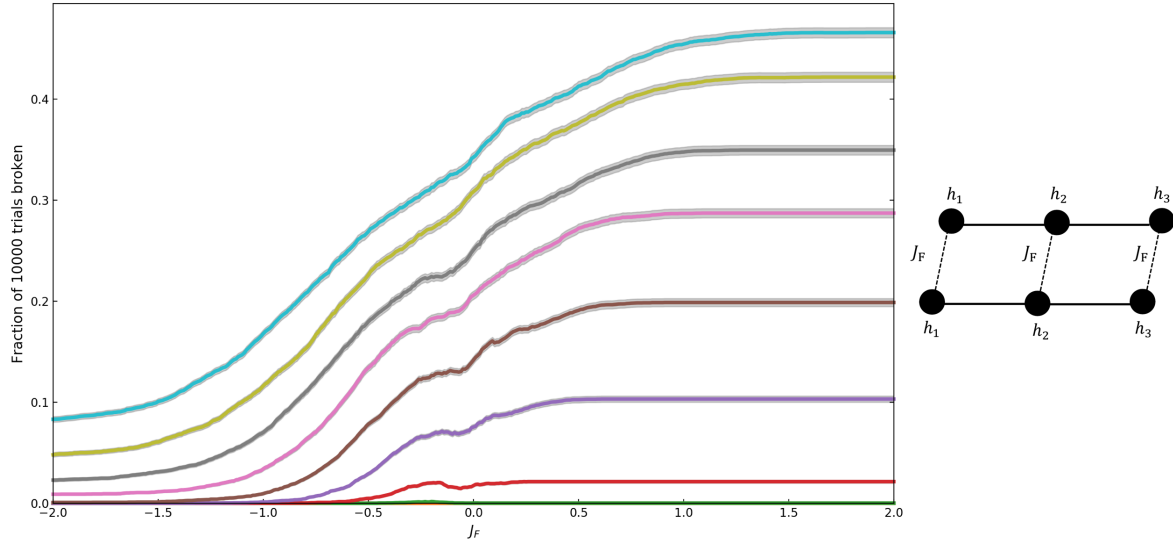


FIG. 6: Left: the fraction of 10000 trials with an incorrect ground state for the $n = 3$ problem instance with 2 duplicates for varying duplicate coupling strength for a range of error bounds: 0.9 at the top down to 0 in steps of 0.1. Uncertainties are the light grey lines. Right: graphical representation of the Ising configuration.

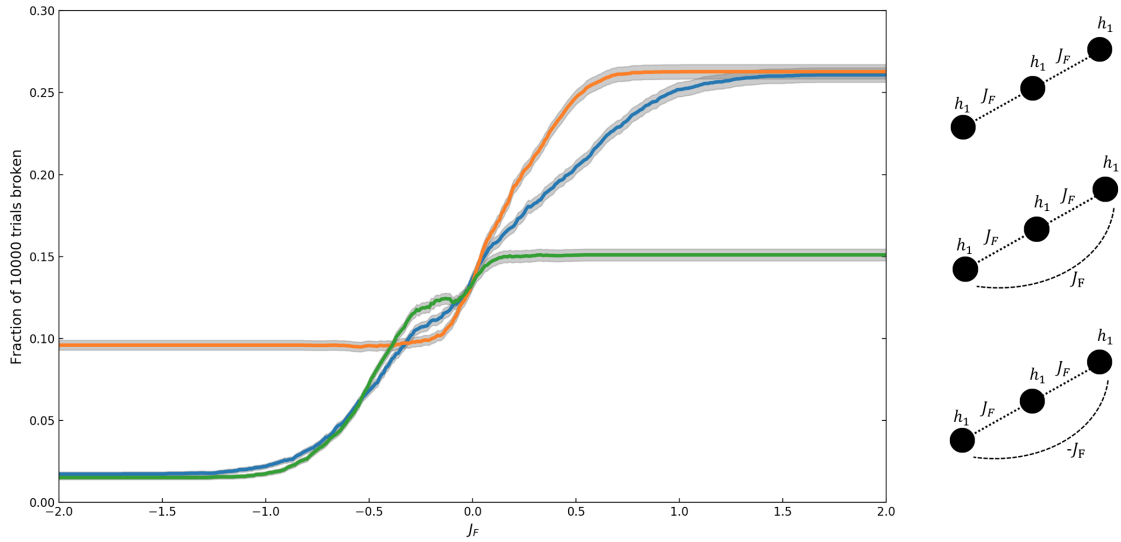


FIG. 7: The fraction of 10000 trials with an error bound of 0.7 with an incorrect ground state with duplicate coupling strength J_F for the $n = 3$ problem instance. For a (blue, top right) a linear chain, (orange, middle right) a ferromagnetic loop, (green, bottom right) an antiferromagnetic loop. Uncertainties are the light grey lines.

the results for a bound of 0.7 are shown. This was the lowest error for which over half the trials of the unprotected instance had a broken ground state and one which captures the differences in behaviour between each different coupling method across the range of error bounds.

An additional copy to the linear chain led to a similar relationship between the fraction of broken trials and duplicate coupling strength, with a steeper transition between limiting values for ferromagnetic and antiferromagnetic couplings, values which were decreased, antiferro-

magnetic more noticeably, such that the best success probability could be obtained for smaller negative values of J_F . With the exception of a small range of negative J_F , the ferromagnetic loop performed worse than the other couplings. Furthermore, it is outperformed by a linear chain for $k = 2$, for example its lowest failure fraction for an error bound of 0.7, 0.095, was greater than the lowest result for the linear chain with one less duplicate, as seen in Table I. The antiferromagnetic loop performed best for the given range of J_F , particularly for negative values. The greatest decrease was by 97% of the fraction of failures from the unprotected instance.

2. *The $n = 5$ maximum independent set instance*

Next, the results from the smaller instances were applied to a larger 5 vertex instance of the maximum independent set problem, as described in Fig. 4. The solution to the $n = 5$ instance corresponds to '10011' or 19. The effect of increasing error ranges on the validity of the ground state can be seen in Fig. 5. With the exception of the lowest errors, this instance saw greater decreases in the fraction of successful trials. The results for a single duplicate are shown in Fig. 8, at higher error bounds the relationship is quite similar to the $n = 3$ instance, but for bounds of 0.4 and below at $-2 < J_F < 0$, there is a spike of failed trials. Relative to the fraction of failures outside this particular range of J_F , this spike is increasingly large for smaller error bounds. Worst affected are the trials with a bound of 0.1, which has a negligible failure rate otherwise. The structure of the increase in failures is clearest for this error bound, with a plateau of greatest failure for $-1.5 < J_F < -0.5$. To try and determine the cause of the spike in failure probabilities, the energy levels of the encoded problem Hamiltonian for the 5 vertex instance with 1 duplicate, $k = 2$, with J_F in the range corresponding to the previously mentioned plateau were observed without errors. The ground state was six fold degenerate, as seen in Fig. 9, with 2 out of the six states failing to correspond to states representing a maximum independent set. This in itself shows that the protection scheme with these specific settings had led to a problem misspecification but wouldn't have been noticed without explicitly checking the Hamiltonian energy levels. Including a small perturbation to the problem parameters in the form of an error in a range bounded by 0.1 led to a breaking of this degeneracy such that a third of the time the global minimum of the problem did not correspond to a maximum independent set, this can be seen in Fig. 8, where the plateau of the spike in errors for a bound of 0.1 approximately equals 0.33.

A similar effect can be observed in Fig. 9 for 2 duplicates although for each choice of coupling the magnitude of the spike was decreased, with it almost disappearing for the ferromagnetic loop. Although this most likely appears to be the case because of the higher baseline fraction of failures for this coupling. In this case the antiferromagnetic loop, despite having the largest spike at small negative J_F , yielded the lowest fraction of failed trials across the range of error bounds, with this occurring at larger negative J_F .

The lowest fraction of trials with a broken ground state can be seen in Table I. A single duplicate sees a reduction of 87%, 2 duplicates a reduction of 89%. Both of these results were with an antiferromagnetic coupling between duplicates and the 2 duplicate case with no additional coupling (as in top right Fig. 7). That the spike in failure probabilities didn't occur

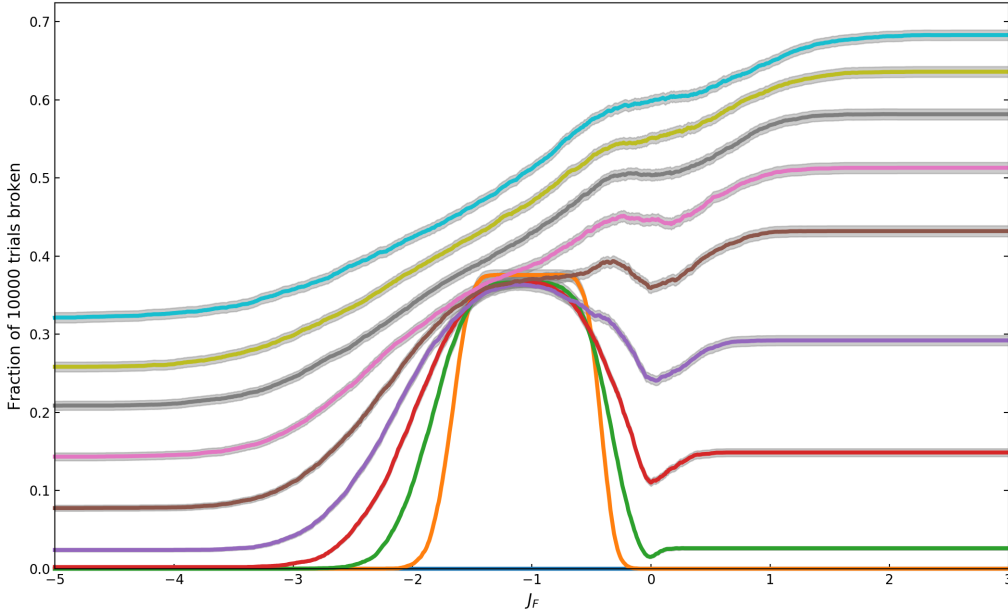


FIG. 8: The fraction of 10000 trials with an incorrect ground state with changing duplicate coupling strength J_F for the $n = 5$ problem instance with 1 duplicate and a range of error bounds: 0.9 at the top down to 0 in steps of 0.1.

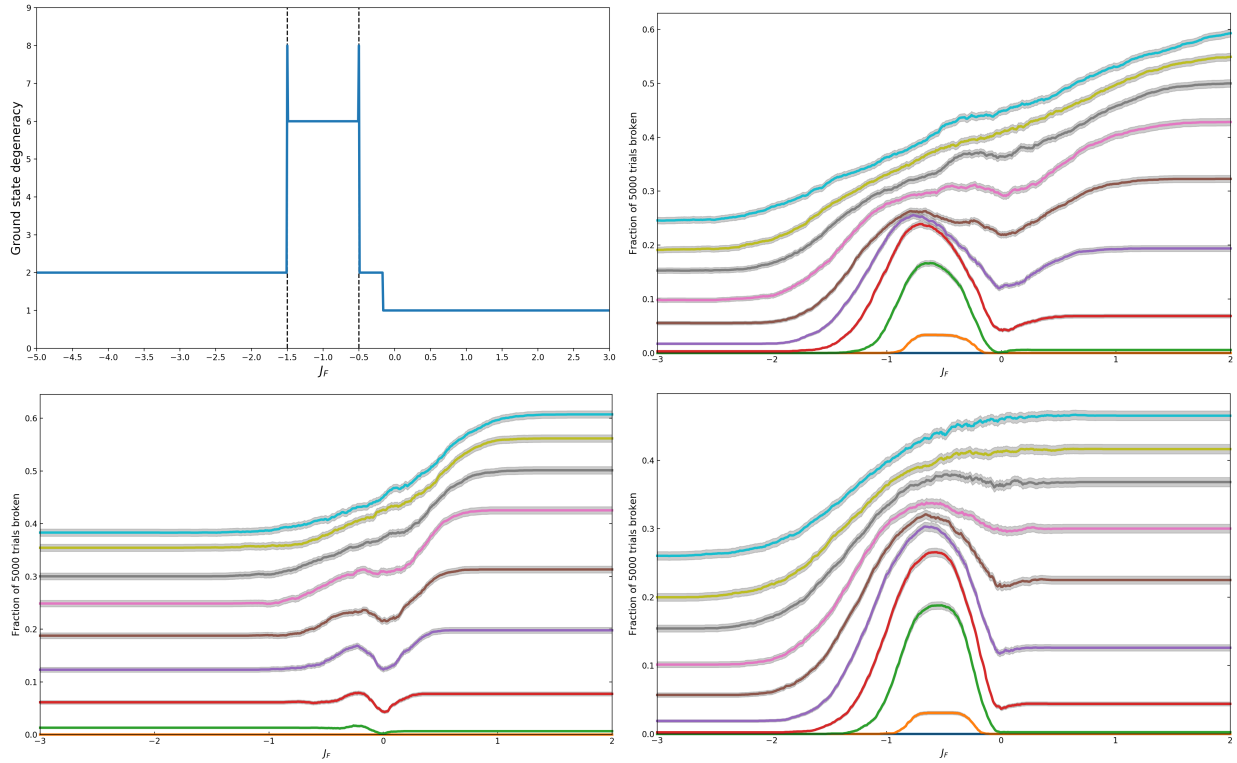


FIG. 9: Top left : ground state degeneracy against duplicate coupling strength J_F for $n = 5$ problem instance with 1 duplicate and an error bound of 0 . The fraction of 5000 trials with an incorrect ground state with changing duplicate coupling strength J_F for the $n = 5$ problem instance with 2 duplicates and a range of error bounds: 0.9 at the top down to 0 in steps of 0.1. Uncertainties are the light grey lines. Top right (linear chain), bottom left (ferromagnetic loop) and bottom right (anti ferromagnetic loop).

with the $n = 3$ instance suggested it could have appeared due to differences in the parameters used to specify the problem instance. Next these parameters were varied in order to see if the spike could be reduced.

3. Problem parameter scaling

It was essential that any problem parameter variation maintained the structure of the problem, with a maximum independent set as the configuration corresponding to the ground state of the problem Hamiltonian. The adjacency matrix of the graph was directly used to define the couplings J_{ij} and used to derive the local fields h_i , scaling the values of this matrix, otherwise 1 or 0, by a constant was a way to maintain the problem structure. Initially, scaling constants of 0.5 and 2 were used with the $n = 5$ instance with 1 duplicate, the effect of these changes can be seen in Fig. 10. The smaller scaling reduces the magnitude of the spike and the range over which it appears, while the larger coupling exacerbates the problem. As the spike has the most distinct effect at an error bound of 0.1, the effect of a range of couplings was observed for this value, as shown in Fig. 11. For very small scaling constants and negative duplicate couplings the problem loses its structure as failure probabilities tend towards 1. There is a very narrow range of problem scaling constants, ~ 0.3 , where the fraction of failed trials is constant. Increasing the scaling beyond this leads to an increased range of J_F for which there is an increase in failures. As can be seen in Fig. 5, an error bound of 0.1 corresponds to an almost negligible increase in trials with a broken ground state for an unprotected problem instance, to see how scaling problem parameters affected trials with a greater magnitude of error, a bound of 0.5 was chosen, as this led to over half the trials failing on the unprotected instance. The results can be seen in Fig. 11, scaling seems to have little effect across the majority of J_F with the exception of very small scaling constants which lead to a decrease in success as in the lower error instance. Interestingly there is a decrease in failure probabilities at higher magnitude negative J_F for a small range of scaling constants. This left triangle where the protection scheme leads to either better or no worse results is present for both error bounds, suggesting there could be a choice of problem scaling constants and duplicate coupling strengths where the protection scheme can be used reliably for a range of error bounds.

B. Solving instances of the maximum independent set with quantum dynamics

1. Adiabatic quantum computing

The previous section was able to confine the effect of misspecification errors to a static context, by simply observing the energy levels of the problem Hamiltonian with respect to the standard computational basis. If it is possible to solve the maximum independent set problem in this way, by simply constructing an Ising Hamiltonian, why would it be necessary to go through the trouble of performing adiabatic time evolution to reach the same Hamiltonian? This necessity comes down to the size of the quantum system used to represent the problem. As mentioned in the background section, for n qubits there are 2^n states, each representing a different measurement outcome, that need to be specified. An Ising Hamiltonian for an n qubit

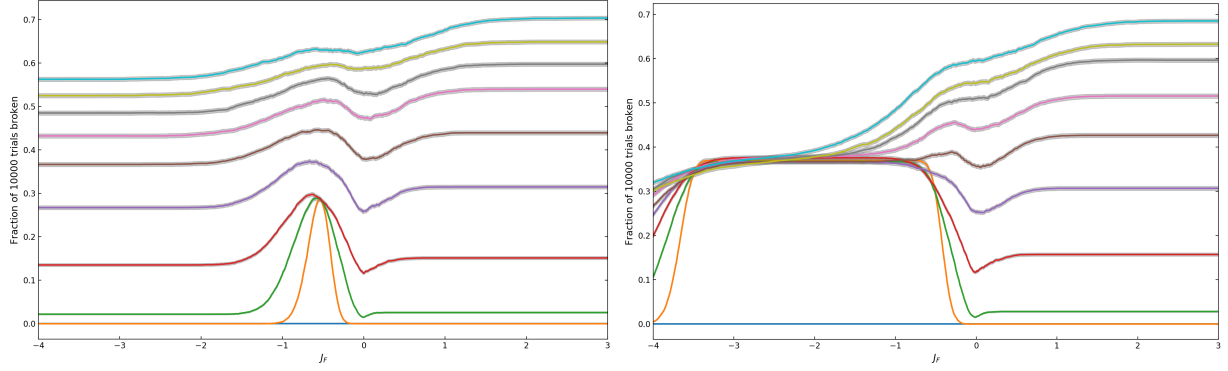


FIG. 10: Fraction of 10000 trials with an incorrect ground state for different 2 duplicate coupling strengths for a range of error bounds: 0.9 at the top down to 0 in steps of 0.1 for a problem parameter scaling of left: 0.5, right: 2. Uncertainties are the light grey lines.

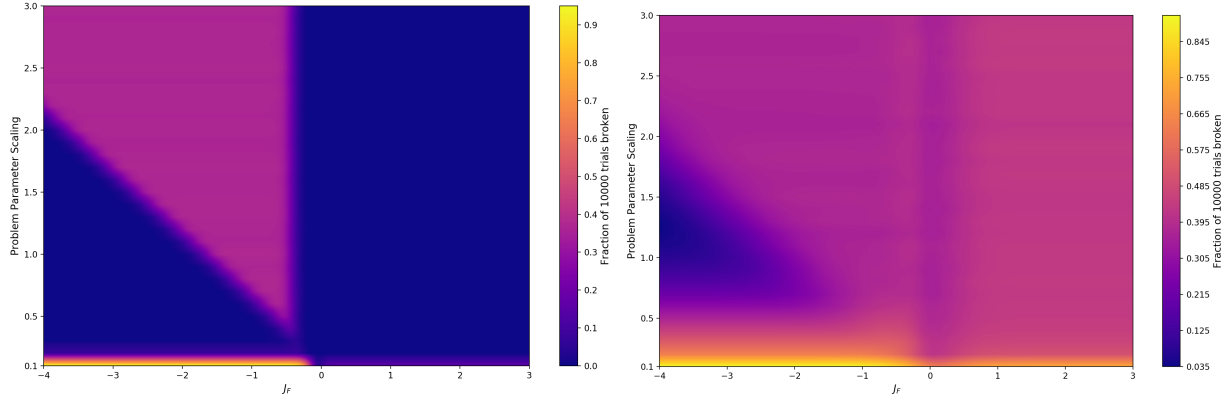


FIG. 11: The fraction of 10000 trials with an incorrect ground state for different 1 duplicate coupling strengths and problem parameter scaling constants for error bounds of left: 0.1, right: 0.5.

n	Error bound	k	Lowest failure fraction	J_F	Loop coupling strength
3	0.7	1	0.512 ± 0.005	-	-
		2	0.023 ± 0.001	-1.99	-
		3	0.015 ± 0.001	-1.29	$-J_F$
5	0.5	1	0.601 ± 0.005	-	-
		2	0.078 ± 0.003	-4.76	-
		3	0.065 ± 0.002	-2.31	0

TABLE I: The lowest failure fractions out of 10000 trials as a result of implementing the protection scheme with k blocks ($k = 1$ corresponds to no protection) with a coupling strength of J_F for problem instances with n vertices. Loop coupling strength refers to the strength of this additional coupling possible with 2 duplicates. Error bounds are the lowest error bound which led to a failure fraction of over 0.5 for trials with no protection scheme.

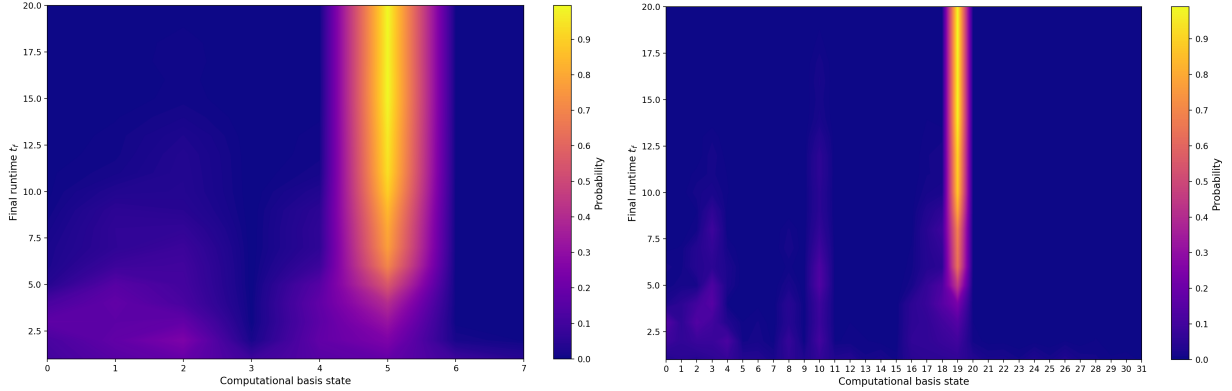


FIG. 12: The probability of being in each computational basis state with increasing final runtime t_f for $n = 3$ (left) and 5 (right) problem instances.

system will be represented by a $2^n \times 2^n$ matrix, so for a 50 qubit system and 32 bit floating point numbers to represent the matrix elements this would require 4×10^{13} exabytes ($(2^{50} \times 2^{50} \times 32)/10^{18}$), much too large for any current computer to store. For solving problems with these larger systems a machine physically implementing adiabatic quantum computing is required. There are far fewer parameters needed to describe a physical system to implement computation: specifying a 50 vertex maximum independent set problem mapped to the Ising model (without any protection scheme) would require 2500 J_{ij} and 50 h_i . It therefore seemed useful to observe the dynamics of adiabatic quantum computing for these small problem instances as they quickly become an important consideration as systems grow to the point where quantum computing shows its advantage over classical.

The results can be seen in Fig. 12. First the $n = 3$ instance was considered. The probability of being in a particular computational basis state, each of which corresponding to a different assignment of weights to the problem instance graph as in Fig. 4, with increasing final runtime. It is important to emphasise this is probability of being in each state for the system at the end of time evolution of Eq. (5), not the change in probabilities during a single run. The algorithm reaches a probability of around 0.99 of being in the expected ground state at a final runtime of $t_f = 16$. The $n = 5$ instance sees a longer t_f required to reach a higher success probability, at the maximum runtime here of $t_f = 20$, the probability of being in the expected ground state is 0.98.

2. Quantum walk

As noted it is possible to use a quantum walk to determine the ground state of an particular Ising model configuration [17]. As a maximum independent set instance can be represented by an Ising Hamiltonian, the quantum walk was used to solve the maximum independent set instances considered in this work. The results can be seen in Fig. 13, unlike with the adiabatic protocol, the success probability oscillates with the final runtime of the algorithm. For the range of final runtimes considered, the maximum success probability and runtimes for the $n = 3$ instance: 0.69 for $t_f = 18.59$, for the $n = 5$ instance 0.48 for $t_f = 23.0735$.

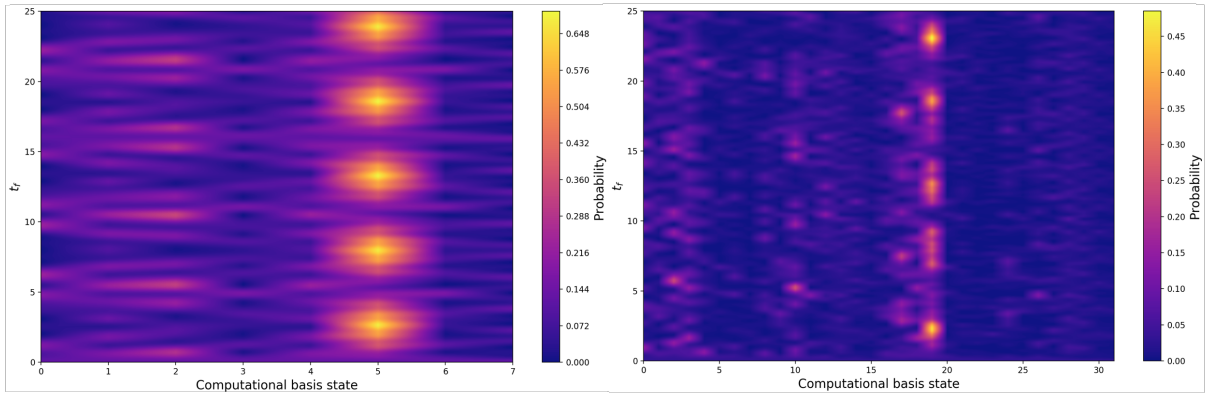


FIG. 13: The probability of the system being in a different basis state with increasing final search time t_f for a quantum walk with 10000 time steps and a hopping rate of 0.715 for $n = 3$ (left) and 0.789 for $n = 5$ (right).

5. DISCUSSION

This thesis has been examining the effectiveness of a scheme to suppress the effect of misspecification errors on the accuracy of an Ising Hamiltonian being used as a problem Hamiltonian for adiabatic quantum computing. This examination has been driven by exploring the performance of the scheme for the maximum independent set problem. The general goal has been assessing the suitability of the scheme as a method for error suppression that only requires local information as this would lend itself to being scalable.

As shown in Fig. 5, the responses of different maximum independent set problem instances to an increasing error bound have a similar form but are of a different magnitude. With both instances, the fraction of trials with incorrect ground states tends towards a limiting value as the error bound increases. At higher error bounds, starting approximately at the size of the largest problem parameters, the energy levels of the problem Hamiltonian are shuffled. Taking into account the degeneracy of energy levels of the problem Hamiltonian, the limiting value is close to the probability of a uniform random choice out of the possible energy levels, but slightly larger due to a level of remaining problem structure.

When the protection scheme is introduced, the specific characteristics of each problem instance lead to quite different results. The $n = 3$ instance responds well to the protection scheme, a single duplicate with antiferromagnetic couplings to the original can bring down the fraction of trials with a broken ground state from over half to 3% (error bound of 0.7). That a negative J_F , corresponding to an antiferromagnetic coupling, performed better than the ferromagnetic case, more so for larger ranges of errors, is interesting as it wasn't an idea proposed in the papers introducing the scheme (although these papers were aiming for every duplicate to remain in the correct configuration). In this work a minimum of one duplicate is necessary for a successful trial, this allows for more freedom in the choice of protection scheme parameters. Increasing the number of duplicates doesn't appear to lead to major differences in the relationship of the fraction of failed trials to J_F , but can bring an additional decrease in this fraction. However, this decrease is dependent on how the additional duplicate is coupled, an antiferromagnetic loop

can lead to a minimum failure probability of around 1.5% while the ferromagnetic loop sees a minimum of around 10%. The results for the ferromagnetic loop are less favourable than for one less duplicate, suggesting that the additional qubit overhead wasn't justified in this case.

The $n = 5$ instance also responded well to the protection scheme with increasing numbers of duplicates, the fraction of trials with a broken ground state was reduced by 87% with one duplicate and 89% with two. However, this positive response was dependent on the choice of encoding parameters. The case with the ferromagnetic loop for $n = 3$, with two duplicates performing worse than one duplicate, still led to improvements over no encoding. Unlike this case, encoding the $n = 5$ instance according to the protection scheme has the potential for worse results than with no protection scheme at all. This can be seen most clearly in the results for one duplicate at $-2 < J_F < 0$. The spike in failure probability corresponds to the range of duplicate coupling strengths where the encoded Ising Hamiltonian without error has a six fold degenerate ground state. Four of the six degenerate states corresponded to a correct maximum independent set solution, two were only independent sets. Once errors were introduced, the degeneracy was broken and roughly a 1/3 of the time the ground state would be a non-maximum independent set. This effect didn't appear for positive J_F , where the ground state corresponded to both blocks being in the expected ground state, it could have been that the specific range of J_F led to a weakening of the maximum independent set conditions in the mapping, for example partially cancelling the energy associated with states with more qubits in $|1\rangle$ as a result of the $\kappa\sigma^z$ term in Eq. (13). Using two duplicates with the $n = 5$ instance didn't lead to significant improvements over one duplicate, but did reduce the presence of the spike in failures.

So it could be concluded, that for some problem instances, with certain levels of error, doing nothing would lead to more favourable results than implementing the error suppression scheme. However, treating not only the parameters used for encoding the protection scheme as variable, but also the parameters defining the problem, was shown to lead to a situation where the protection scheme helped, or at worst did nothing, for multiple error bounds. This can be seen in Fig. 11 in the triangular region on the left in both plots. The choice of scaling constant introduces another parameter that requires careful choice in its assignment. Comparison of Fig. 8 with Fig. 10 shows that although scaling the problem parameters down led to a reduction in the magnitude of the spike in failure probabilities, it led to an increase in failure probabilities across the range of J_F and error bounds. That the negative effects of a problem instance not responding well to the error suppression scheme could be mitigated is encouraging, however, the requirement to scale every problem parameter to do so could be considered to weaken the claim that the scheme only requires local information to be effective.

The same number of additional qubits are required to go from $k = 1$ to $k = 2$ and $k = 2$ to $k = 3$, however, there is not the same magnitude in decrease in failure probability, as seen in Table I. This suggests that there might be diminishing returns on further increasing the size of the system with further redundant qubits for encoding. It is possible higher numbers of duplicates are more suited for applications that require a very high fidelity and are looking to maximise the use of available qubits.

The results for the $n = 5$ instance reinforce the idea that, if not chosen carefully, the protection scheme parameters could lead to worse behaviour over even the unprotected problem with errors present. What is exactly meant by 'carefully' constitutes one of the primary questions that arose during the work for this thesis. How to choose the protection scheme parameters for a given

problem instance such that the problem remains defined as intended and the scheme doesn't become a source of misspecification errors?

The generality of the statements that can be made in this work are limited due to the small range of problem instances looked at. Extending this range and seeing if the same behaviour appears and for what encoding parameters would be a possible next direction for developing a more quantitative explanation for this problem misspecification by the protection scheme. An explanation that could be necessary if this scheme is to be scaled up to larger, arbitrary problem instances.

Through simulating quantum dynamics adiabatic quantum computing was able to reach the optimal solution for these small instances of the maximum independent set problem. Simulating these dynamics with a problem Hamiltonian subject to misspecification errors could lead to a non-optimal solution. Although, this was not due to a failure in the quantum dynamics, which were reaching the ground state of the problem Hamiltonian, but because this Hamiltonian no longer accurately reflected the specific problem instance. Whether the protection scheme remains effective in the more physically realistic situation of adiabatic evolution subject to external noise is another interesting question. Simulation of a quantum walk was shown to be able to solve the problem instances considered, although with lower success probabilities than those achieved by adiabatic quantum computing. These probabilities could be improved through multiple repeats runs of the quantum walk algorithm [17].

6. CONCLUSIONS

This thesis has demonstrated that it is possible to solve instances of the maximum independent set problem using simulated adiabatic quantum computing. Furthermore, when the Hamiltonian encoding these problem instances is subjected to misspecification error, the protection scheme presented generally succeeds in suppressing the magnitude of the effect of these errors. However, it was shown that it is possible for the scheme itself to lead to misspecification errors. This occurred in specific cases: the $n = 5$ problem instance, with $-2 < J_F < 0$. The error bounds for which this had the most notable effect were such that, with no protection scheme used, a minority of trials had a broken ground state and subsequently the encoding led to worse results. Although this misspecification could be avoided with different J_F or further duplicate blocks, the lack of a link to the specific property of the problem instance causing the error meant the question of how to choose effective encoding parameters for an arbitrary instance remains open. Determining these specific properties could lead to the possibility of more general claims to be made about the protection scheme, as it could be observed if graphs with similar properties exhibited similar behaviour. The scaling of the parameters used to define the problem was shown to be able reduce the impact of this protection scheme introduced misspecification but, as this involved modifying the entire problem, it could be considered to limit the potential of this scheme as a scalable solution for error suppression which requires only local information to be effective.

For both problem instances, the scheme was shown to be effective in reducing the impact of the swapping of energy levels as a result of perturbations to the problem parameters. It was most effective when using antiferromagnetic couplings between duplicates, which hadn't been

previously considered. The $n = 3$ instance saw a reduction of fraction of trials with an incorrect ground state of 97% and the $n = 5$ instance of 89%. Higher reductions could be obtained by using additional duplicates although two difficulties obstructed further detailed examination. First, the system size became too large to simulate for a large number of trials. Second, with additional duplicates came a greater set of ways to couple these duplicates together, the choice of which was shown to affect the effectiveness of error suppression. Exhaustively testing the different choices wouldn't be practical considering the first difficulty. A next step in this direction would be to observe the results of the protection scheme with a wider range of small size problem instances with numbers of duplicates similar to that considered in this work.

In the encoding scheme each individual physical qubit is duplicated to form a logical qubit. In this work this duplication was done in the same way for every original physical qubit. Instead, tailoring the parameters of duplication to each physical qubit, and doing so based on local information: the strength and number of the couplings to neighbouring qubits and local field strengths, would lead to a scheme more suited to scaling to larger system sizes.

As the suppression scheme introduces an overhead of additional qubits, knowing how to use these in the most effective manner possible for a given problem will be increasingly important as larger sizes are considered. The protection scheme has shown to be effective for the problem instances looked at. It will be necessary to consider a wider range of problem instances in order to explain and extend the work done in this thesis, so as to truly assess the scheme as a viable choice for suppressing the effects of misspecification errors in a scalable manner.

Acknowledgments

The author would like to thank Jemma Bennet for very useful discussions comparing results and Shirin Ermis for invaluable advice on writing style and structuring.

References

- [1] Powell J. R., *The Quantum Limit To Moore's Law*, Proc. IEEE (2008), Vol. 96, No. 8, p. 1247-1248.
- [2] Shor P. W., *Polynomial-Time Algorithms for Prime Factorization and Discrete Logarithms on a Quantum Computer*, SIAM Journal on Computing, Oct. 1997, Vol. 26, No. 5, p. 1484-1509.
- [3] Grover L. K., *A Fast Quantum Mechanical Algorithm For Database Search.*, Proc. of the twenty-eighth annual ACM symposium on Theory of Computing, Philadelphia, PA, USA: ACM (1996), p. 212-219.
- [4] C C. McGeoch, R Harris, S P. Reinhardt, P Bunyk, *Practical Annealing-Based Quantum Computing*, 2019, [https://www.dwavesys.com/sites/default/files/14-1036A-B_wp_Practical_Annealing-Based_Quantum_Computing\(1\).0.pdf](https://www.dwavesys.com/sites/default/files/14-1036A-B_wp_Practical_Annealing-Based_Quantum_Computing(1).0.pdf) as of Feb. 2020.
- [5] Lucas A., *Ising formulations of many NP problems*, Front. Phys., Feb. 2014, Vol. 2.
- [6] Benioff P., *The Computer as a Physical System: A Microscopic Quantum Mechanical Hamiltonian Model of Computers as Represented by Turing Machines*, Journal of Statistical Physics, 1980, Vol. 22, No. 5, p.563 - 591.

- [7] Benioff P., *Quantum Mechanical Hamiltonian Models of Turing Machines*, Journal of Statistical Physics, 1982, Vol. 29, No. 3, p.515-546.
- [8] Deutsch D., *Quantum Theory, The Church-Turing principle and the universal quantum computer*, Proc. Roy. Soc. (1985), **A400**, p. 97-117.
- [9] Feynman, R., *Simulating physics with computers*, International Journal of Theoretical Physics. 1982. 21, 6&7, 467488.
- [10] Bennett C. H., Bernstein E., Brassard G., Vazirani U., *Strengths and Weaknesses of Quantum Computing*, SIAM Journal on Computing, Oct. 1997, Vol. 26, No. 5, p. 1510-1523.
- [11] Schumacher B., *Quantum Coding*, Phys. Rev. (1995), **A51**, p. 2738-2747.
- [12] Vandersypen L. et al., *Experimental realization of Shor's quantum factoring algorithm using nuclear magnetic resonance*, Nature, 2001, Vol. 414, p. 883-887.
- [13] DiCarlo L. et al., *Demonstration of two qubit algorithms using a superconducting quantum processor*, Nature, 2009, Vol. 460, p. 240-244.
- [14] Aharonov D., Ambainis A., Kempe J., Vazirani U., *Quantum Walks on Graphs*, Proc. of ACM Symp. on Theory of Comp. (STOC'01), July 2001, p. 50-59.
- [15] Farhi E. and Gutmann S., *Quantum computation and decision trees*, Phys. Rev. (1998), **A58**, p. 915.
- [16] Morley J. G., Chancellor N., Bose S., Kendon V., *Quantum search with hybrid adiabatic-quantum walk algorithms and realistic noise*, Phys. Rev. (2019), **A99**, 022339
- [17] Callison A., Chancellor N., Mintert F., Kendon V., *Finding spin glass ground states using quantum walks*, New J. of Phys, Dec. 2019, Vol. 21.
- [18] Childs. A. M., *Universal computation by quantum walk*, Phys Rev. Lett. (2009), Vol. 102, 180501.
- [19] Farhi E., Goldstone J., Gutmann S., and Sipser M., *Quantum computation by adiabatic evolution*, (2000), arXiv:quant-ph/0001106.
- [20] Santoro G., Tosatti E., *Optimization using quantum mechanics: quantum annealing through adiabatic evolution*, J. Phys. A: Math Gen., 2006, Vol. 39, p. 393.
- [21] Welsh D. J. A., *Codes and Cryptography*, Oxford University Press, New York, 1988.
- [22] W. J. Wootters, W. H. Zurek., *A single quantum cannot be cloned*, Nature, Vol. 299, p.802-803, 1982. Cambridge, Cambridge University Press, 2010.
- [23] Laflamme R, Knill E., *A theory of quantum error correcting codes*, Phys. Rev. Lett., 2000, Vol. 84, p. 2525 - 2528
- [24] Shor P. W., *Scheme for reducing decoherence in quantum memory*, Phys. Rev., Oct. 1995, **A52** , No. 4.
- [25] Calderbank A. R., Shor P. W., *Good quantum error correcting codes exist*, Phys. Rev., 1996, **A54**, No. 2., p.1098 - 1106.
- [26] Steane A., *Multiple particle interference and quantum error correction*, Proc. Roy. Soc. Lond., 1996, **A452**, p.2551.
- [27] Gottesman D., *A class of quantum error-correcting codes saturating the quantum Hamming bound*, Phys. Rev., 1996, **A54**, p.1862.
- [28] Roffe J., *Quantum Error Correction: An Introductory Guide*, Contemporary Physics, 2019, 0010-7514.
- [29] OGorman J., Campbell E. T., *Quantum computation with realistic magic state factories*, (2016),

- arXiv:1605.07197.
- [30] Childs A., Farhi E., Preskill J., *Robustness of adiabatic quantum computation*, Phys Rev., 2002, **A65**.
 - [31] Jordan S. P., Farhi E., Shor. P, *Error correcting codes for adiabatic quantum computation*, Phys Rev., 2006, **A74**.
 - [32] Young K., M. Sarovar., *Error suppression and error correction in adiabatic quantum computation I: techniques and challenges*, Phys. Rev. X., 2013, Vol. 3, Iss. 4.
 - [33] Pudenz K., Albash T., Lidar D., *Error corrected quantum annealing with hundreds of qubits*, Nature Comm., 2014., Vol. 3, p.3243.
 - [34] Young K., Blume-Kohout R., Lidar D., *Adiabatic quantum optimization with the wrong Hamiltonian*, Phys. Rev., 2013, **A88**, Iss. 6.
 - [35] Kendon V., *Decoherence in quantum walks - a review*, Math Struc. in Comp. Sci., 2007, Vol. 17, No. 6 , p. 1169.
 - [36] Chancellor N., *Quantum optimization and applied algorithms*, Undergraduate Level 3 Project Script, May 15 2019.
 - [37] Choi V., *Adiabatic Quantum Algorithms for the NP-Complete Maximum-Weight Independent Set, Exact Cover and 3SAT Problems*, 2010, arXiv:quant-ph/1004.2226.
 - [38] Dickson N. G., Amin M. H. S., *Does Adiabatic Quantum Optimization Fail for NP-complete Problems?*, Phys. Rev. Lett., 2011, Vol. 106, No. 5, p. 050502.
 - [39] Yarkoni S., Plaat A., Bäck T., *First results solving arbitrarily structured Maximum Independent Set problems using quantum annealing*, 2018 IEEE Congress on Evolutionary Computation (CEC), Rio de Janeiro, 2018, pp. 1-6.
 - [40] E. Jones, T. Oliphant, P. Peterson, et al., *SciPy: Open source scientific tools for Python*, 2001, <https://www.scipy.org/> as of April 2020.

A. CALCULATION OF UNCERTAINTIES

Here the method for calculating the uncertainty in the fraction of trials with a broken ground state will be described. During these trials the fraction of trials with the correct ground state was calculated, and the complement was taken when plotting these results. This fraction is the mean number of N trials with a correct ground state, so the uncertainty in this value is the standard error:

$$\alpha = \frac{\sigma_{N-1}}{\sqrt{N}}, \quad (18)$$

where σ_{N-1} is the standard deviation of the results from N trials and was calculated:

$$\sigma_{N-1} = \sqrt{\frac{1}{N-1} \sum_{i=1}^N d_i^2}, \quad (19)$$

and $d_i = x_i - \bar{x}$ is the deviation of the i th data point from the mean \bar{x} .

The error was calculated after the average had been calculated. In order to avoid repeat simulations, an expression for the standard error on each result was derived from observing the possible outcomes of each data point. Successful and unsuccessful trials would yield 1 and 0 respectively. Denoting the fraction of successful trials F , it can be seen this value also corresponds to the mean number of correct trials, $\bar{x} = F$. So the deviations from mean for successful and unsuccessful trials were $d_i = 1 - F$ and $d_i = -F$ respectively. Denoting the number of trials with a correct and incorrect ground state as N_1 and N_0 respectively, $N_1 = NF$ and $N_0 = N(1 - F)$. So the sum over squared deviations becomes:

$$\sum_{i=1}^N d_i^2 = NF(1 - F)^2 + N(1 - F)(-F)^2, \quad (20)$$

and the standard error can be calculated:

$$\alpha = \sqrt{\frac{NF(1 - F)^2 + N(1 - F)(-F)^2}{N - 1}}. \quad (21)$$

Setting $F \rightarrow 1 - F$ leads to the same expression and gives the result for the number of trials with an incorrect or broken ground state.

B. SUPPLEMENTARY FIGURES

In Fig. 14 the full plots of the fraction of trials with an incorrect ground against duplicate coupling strength J_F for 2 duplicates, $k = 3$, are shown.

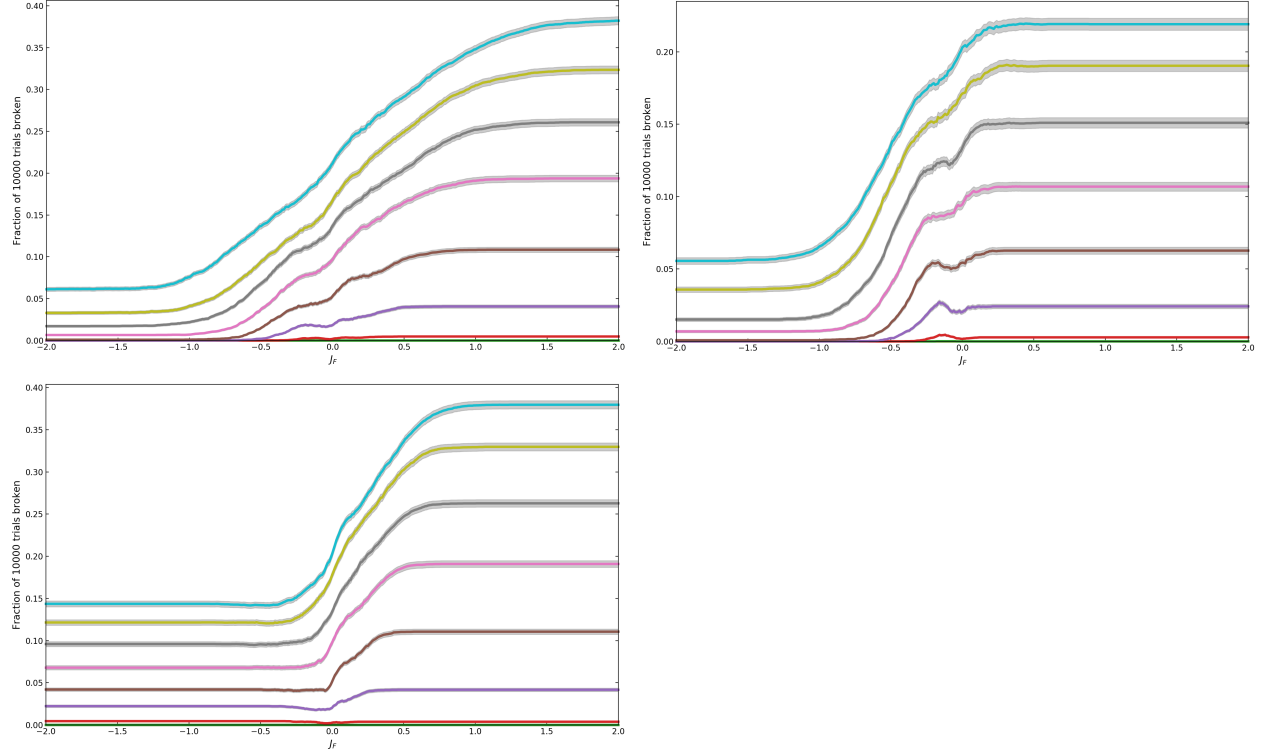


FIG. 14: The fraction of 10000 trials with an incorrect ground state with changing duplicate coupling strength J_F for the $n = 3$ problem instance with 2 duplicates and a range of error bounds: 0.9 at the top down to 0 in steps of 0.1. Uncertainties are the light grey lines. Top left (linear chain), bottom left (ferromagnetic loop) and top right (anti ferromagnetic loop).